

# Polarization switching and relaxation dynamics of bismuth layered ferroelectric thin films: Role of oxygen defect sites and crystallinity

Ji Hye Lee, Ran Hee Shin, and William Jo\*

*Department of Physics, Ewha Womans University, Seoul 120-750, Republic of Korea*

(Received 2 February 2011; revised manuscript received 13 June 2011; published 22 September 2011)

Influence of oxygen vacancies and crystallinity on polarization switching and relaxation dynamics of  $\text{Bi}_{3.15}\text{Nd}_{0.85}\text{Ti}_3\text{O}_{12}$  (BNT) thin films on Pt electrodes have been studied by piezoresponse force microscopy (PFM). Heat treatment of the study induced oxygen vacancies in  $\text{Bi}_2\text{O}_2^{+2}$  layers not in  $\text{TiO}_6^{-8}$  octahedra and changes in crystallinity of the films. Oxygen atoms have two different locations unique in the bismuth layered ferroelectrics and, in particular, the oxygen vacancies at the  $\text{Bi}_2\text{O}_2^{+2}$  layers turned out to be critical for retention of polarization states. Perfect crystallinity in the arrangement of atoms through  $c$ -axis is surprisingly found to sustain polarization switching. Electrostatics of the bound charges in the films with oxygen deficiency and imperfectness of crystallinity are presented in a dynamic model with random-walk motion of point defects and a diffusive migration of mobile and bound charges and their clusters. For the stretched exponential decay of the bound charges in the films, the scaling exponents are 0.086 and 0.289 for well crystalline-thin films.

DOI: [10.1103/PhysRevB.84.094112](https://doi.org/10.1103/PhysRevB.84.094112)

PACS number(s): 77.80.-e

## I. INTRODUCTION

Switching and relaxation of ferroelectric polarization are imperative issues to study the materials as well as to apply them for electronic devices.<sup>1-5</sup> When polarization of ferroelectric materials is studied, it is necessary to consider not only bound charges but also free charges. It is also required to study several problems such as imprint, leakage current, fatigue, and piezoresponse of ferroelectric thin films with many defects.<sup>6-9</sup> As we previously demonstrated in earlier reports, many ferroelectric materials follow unique temporal dependence of polarization decays.<sup>10</sup> The bound charges are undoubtedly related to the ferroelectric spontaneous polarization, whereas the origin of free charges is not obvious. Oxygen vacancies and extra electron or hole carriers are possible candidates, but their conduction mechanism in ferroelectric materials is not yet fully understood.<sup>11</sup> Generally defect charges such as oxygen vacancies existing inside ferroelectric materials or near electrodes could induce fatigue failures in the ferroelectric materials.<sup>12-16</sup> Noguchi *et al.* reported systematic results that oxygen vacancies could cause domain clamping, high-leakage current, and ferroelectric properties.<sup>17-20</sup>

Among the ferroelectric materials for potential device applications, bismuth layer-structured ferroelectrics have been regarded as promising materials for ferroelectric memories and piezoelectric devices operating at high temperatures due to its large spontaneous polarization and high Curie temperature.<sup>21</sup> Thin films of Nd-substituted bismuth titanate (BNT) show a large remnant polarization value ( $\sim 100 \mu\text{C}/\text{cm}^2$ ) compared to other bismuth layered titanates doped by rare earth, as reported by Chon *et al.*<sup>22,23</sup> Owing to the large remnant polarization, BNT is promising for nonvolatile electronic devices, but its relaxation of polarization is not often reported. Figure 1 shows a unit cell of bulk BNT structure. It was suggested that oxygen vacancies might be preferably present in the vicinity of the Bi ions at the  $\text{Bi}_2\text{O}_2^{+2}$  layers for a bulk  $\text{Bi}_4\text{Ti}_3\text{O}_{12}$  (BTO) from x-ray photoemission spectroscopy (XPS) measurements.<sup>12</sup> As BNT belongs with the bi-layered titanate structure group, the materials have two parts: the perovskite structure and  $\text{Bi}_2\text{O}_2^{+2}$  layers in-between the perovskites.<sup>12</sup> The oxygen vacancies

could exist in both of the two parts in Fig. 1. Therefore, it is interesting to investigate the roles of the parts on polarization reversal and charge relaxation.

It was known that the electrical characteristics of bismuth-layered titanates show a strong anisotropic property originating from the layered structure. Their ferroelectricity arises mainly in the perovskite structures in bismuth titanates single crystal.<sup>18</sup> However, in thin films system, there are not sufficient experimental and theoretical approaches to prove enhancement of ferroelectricity between the two oxygen possibilities.

In this paper four BNT samples were grown to have different oxygen contents or crystallinity states. Effect of oxygen vacancies and crystalline quality on charge relaxation was examined by piezoresponse force microscopy (PFM). The poling schemes which were already demonstrated in our earlier reports show its capability in this study of BNT films.<sup>24,25</sup>

## II. EXPERIMENTS

Metal-organic solution with a nominal ratio of 3.15/0.85 for Bi/Nd atoms was coated by a sol-gel method on Pt/Ti/SiO<sub>2</sub>/Si (100) substrates. Coated solution was spun at 3000 rpm and dried at 350 °C for 7 min. The films were crystallized by firing for 20 min in a tube furnace. The thin films annealed at 800 °C in a N<sub>2</sub> (80%)/O<sub>2</sub>(20%) mixture with atmospheric pressure ( $P_{\text{O}_2} = 0.02$  MPa) and in a fully oxygenated ambient ( $P_{\text{O}_2} = 0.1$  MPa) are designated as Films A and B, respectively. The films annealed at 900 °C in the same ambient conditions are called Films C and D, respectively. This is summarized in Table I. The thickness of the films is approximately 300 nm. Although the final firing temperature was somewhat high we could get nonreactive interface of BNT thin films since there were no reaction phases from x-ray diffraction (XRD) or protrusions in the surface morphology confirmed by scanning electron microscopy.

The films were analyzed at room temperature by XRD in a  $\theta$ - $2\theta$  mode scan using Cu  $K\alpha$  radiation (Bruker New D8 Advance). X-ray rocking curve measurement was performed to evaluate the orientation of the thin films. X-ray photoemission

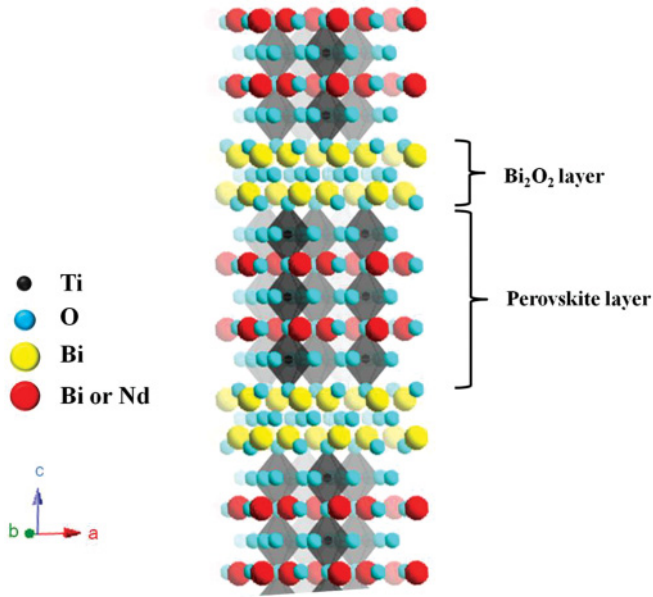


FIG. 1. (Color online) Atomic structure of bismuth titanates with Nd addition. Light, large symbol represents Bi in  $\text{Bi}_2\text{O}_2^{+2}$  layers; dark, large symbol stands for Bi or Nd in the perovskite  $(\text{Bi,Nd})_2\text{Ti}_2\text{O}_{10}^{-2}$ . Light, small symbol represents O; dark, small symbol stands for Ti. This structure represents a bulk sample without any defects or vacancies, but it is useful to take this structure for locating oxygen defects and possible breakage of Ti-O bonding.

spectroscopy (XPS) in the BNT thin films was investigated to identify which chemical binding of metals with oxygen lost oxygen during the oxygen-deficient annealing process. XPS was performed using a monochromatic Al  $K\alpha$  source (1486.6 eV) with an instrumental resolution of  $\sim 0.4$  eV (Omicron EA 125 hemispherical). Macroscopic  $P$ - $E$  curves were measured by a TF analyzer with 300- $\mu\text{m}$  top Pt dots.

Local polarization was observed by a dynamic-contact mode of PFM (Nanofocus Inc., n-Tracer), which was operated with amplitude 0.4 V (peak-to-peak) and frequency 70 kHz using Pt/Ir-coated Si cantilevers. A reverse-poling scheme is used in this paper to examine effects of the asymmetric structure on charge distribution of ferroelectric capacitors.<sup>25</sup> In the preceding few decades many researchers have studied local properties of ferroelectric thin films using scanning probe microscopy (SPM). Through this technique the direct information of domain dynamics and visualization of ferroelectric domains could be known. Therefore the effect of oxygen vacancies and crystalline quality on charge relaxation by PFM has been examined. In order to clarify effects of the asymmetric structure on charge distribution of the ferroelectric capacitors,

a reverse poling scheme was applied. The domain images were acquired every 4 min in the course of two-hour measurements. Scanned images of piezoresponse were carefully treated with a fresh and robust Pt-metal tip for each set of data.

### III. RESULTS

Figure 2(a) shows XRD  $\theta$ - $2\theta$  patterns of the BNT thin films. All the films show (117) of the BNT phase, which is a signature of polycrystalline-textured films. Here, crystallinity means the structural perfectness in the BNT films which show (00 $l$ ), (117), and (200) peaks. Films A and C grown in a  $\text{N}_2(80\%)/\text{O}_2(20\%)$  mixture with atmosphere pressure ( $P_{\text{O}_2} = 0.02$  MPa) on different annealing temperatures have weak (00 $l$ ) peaks, while the samples grown fully oxygenated show other (00 $l$ ) and (111) reflections as well as (117) and (200) peaks. This is an interesting imperfectness in crystallinity, because the layered nature of BNT usually brings out (00 $l$ ) reflections parallel to the substrate.<sup>26</sup> Lacking the  $c$ -axis peaks but still having strong (117) and (200) peaks may indicate that the films may be mixed with well-crystalline and poor-crystalline parts simultaneously. The improvement of crystallinity owing to the increasing of the annealing temperature is observed in Fig. 2(a). Figure 2(b) shows the rocking curves for the (008) reflection of Films B and D. The rocking curves of the (117) peak of all the thin films are shown in Fig. 2(c). Areal values under the rocking curves indicate the amount of grains with direction, suggesting Films B and D have much more crystalline grains than Films A and C. Oxygen deficiency in the thin films is also a factor to determine their crystallinity and is related to the result of their ferroelectric properties and the relaxation of polarization states in each film measured by PFM. Films B and D might have less oxygen vacancies than Films A and C. From these results it is probable that crystallinity is improved by decreasing oxygen deficiency and increasing the annealing temperature of the films.

It is well known that the annealing temperature is important to crystallize ferroelectric thin films during sol-gel deposition process.<sup>27</sup> All the four BNT thin films consist of a single-phase, bismuth-layered  $\text{Bi}_4\text{Ti}_3\text{O}_{12}$ -type structure. There are no pyrochlore peaks appearing in the thin films annealed at a lower temperature<sup>28,29</sup> than the annealing condition in this experiment.

The lattice constants have been calculated from the XRD patterns and listed in Table II using a refinement program, Topas (Bruker). The result showed that, due to vaporization of Bi, the unit cell volume decreased while annealing temperature increased when compared between Films A and C or Films B and D. When we compared oxygen fully ambient atmosphere effects on the lattice parameters, it has been known that

TABLE I. Synthesis conditions and ferroelectric properties of BNT samples.

Sample	Thin-film growth conditions	$2P_r$ ( $\mu\text{C}/\text{cm}^2$ )	$E_c^+$ (kV/cm)	$E_c^-$ (kV/cm)
Film A	Firing in a furnace: 800 °C for 20 min in air ( $P_{\text{O}_2} = 0.02$ MPa)	13.8	97.0	113.7
Film B	Firing in a furnace: 800 °C for 20 min in air ( $P_{\text{O}_2} = 0.1$ MPa)	17.1	97.0	113.7
Film C	Firing in a furnace: 900 °C for 20 min in air ( $P_{\text{O}_2} = 0.02$ MPa)	34.7	108.2	124.8
Film D	Firing in a furnace: 900 °C for 20 min in air ( $P_{\text{O}_2} = 0.1$ MPa)	35.8	108.2	124.8

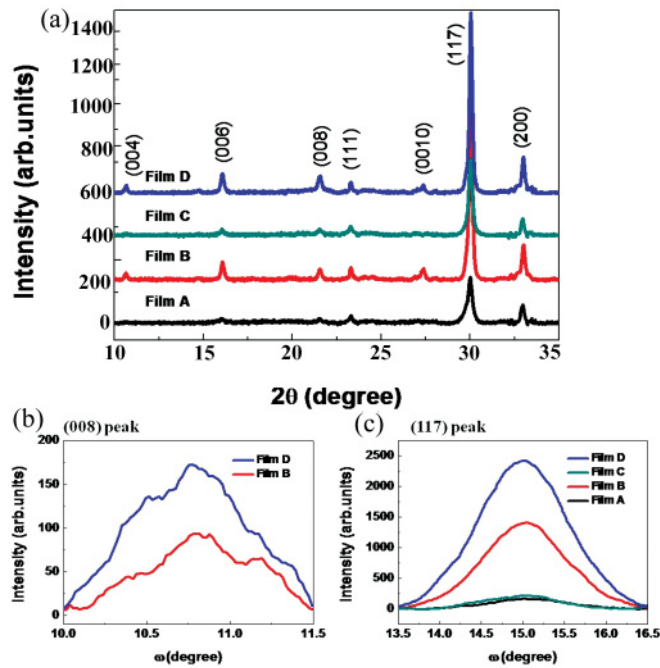


FIG. 2. (Color online) (a) XRD patterns of four different BNT samples. The diffraction patterns obtained by  $\theta$ - $2\theta$  scans show relative ratios of  $(00l)$  reflections as well as  $(117)$  and  $(200)$  orientations. It is very likely that according to the annealing conditions, texturing and oriental distribution of the BNT grains are varied. (b) X-ray rocking curves for  $(008)$  reflection of Films B and D. (c) X-ray rocking curves for  $(117)$  peak of Films A, B, C, and D.

the samples with more oxygen deficiency showed a larger volume of unit cells than that of the thin films with less oxygen deficiency. In the case of V- and W-doped bismuth titanates, there is no change of lattice parameters between the sample with more oxygen deficiency and the sample with less oxygen deficiency compared with the lattice parameters of La-substituted bismuth titanates (BLT) where  $a = 52.28$ ,  $b = 54.18$ , and  $c = 32.90$  Å because of the low-doping content of vanadium ( $x = 0.012$ ) and tungsten ( $x = 0.015$ ), respectively.<sup>18</sup> However, in our case the amount of doped-Nd ions ( $x = 0.85$ ) is enough to distort unit cell structure.

Figure 3 shows the macroscopic polarization vs applied voltage loops of BNT thin films. Remnant polarization ( $2P_r$ ) of Film A was  $13.75$  and Film B was  $17.10$   $\mu\text{C}/\text{cm}^2$ ; remnant polarization for Films C and D was  $34.74$  and  $35.83$   $\mu\text{C}/\text{cm}^2$ , respectively. The coercive field ( $2E_c$ ) of Films A and B was  $201.7$  kV/cm. Films C and D show higher coercive field, approximately  $233$  kV/cm more than that of Films A and B. It was suggested that a small enhancement of  $P_r$

observed in BNT under high-oxygen ambient is attributed to domain depinning attributable to oxygen deficiencies. There was not any significant difference compared with oxygen existence, but apparently large remnant polarization and well-saturated ferroelectric switching behaviors come up with high annealing temperature. Noguchi *et al.* have reported that the enhancement of a remnant polarization value in BTO single crystals was fabricated in different oxygen pressure. A BTO single crystal with more defects showed lower remnant polarization than that with standard or less defects because oxygen vacancies play a role to suppress remnant polarization by the clamping of the domain walls.<sup>30,31</sup>

Figure 4 shows an as-grown state of the four BNT thin films by PFM measurements. Structural imperfections associated with polycrystalline nature of the BNT thin films result in spatial variations of local switching at the nanoscale level in Fig. 4. Local hysteresis loops were obtained in two different spots of Films B, C, and D in Figs. 4(d), (f), and (h), respectively. These are distinguished by different switching characteristics such as built-in potential and coercive field, which are very different from the values of the  $P$ - $E$  loops measured macroscopically in Fig. 3. PFM measurement could give us direct information on local charge distribution, domain-wall interaction with defects, and domain dynamics during phase transition of ferroelectric thin films. Application of PFM to the electrical characterization of individual nanocapacitors has revealed remarkable variations in their switching behaviors, evidently due to the inhomogeneity of polycrystalline thin films and electrodes at the nanoscale level.<sup>32-34</sup> Randomly oriented ferroelectric domains in the PFM images were shown not only in polycrystalline thin films but also in epitaxial thin films at nanoscale. The arrows 1 and 2 show acute difference of contrast, indicating that as-grown polarization states are aligned with opposite direction between the two regions. Note that the interpretation of PFM hysteresis loop is to some extent different from the meaning of macroscopic  $P$ - $E$  loops. In PFM measurements scanning speed is much slower than macroscopic measurement, and mechanical response is inherently included in their operation. Thus, it is not easy to compare those two results directly, but it is still worthwhile to get PFM loops owing to their locality of physical properties obtained.

In Fig. 5 PFM images of the BNT thin films with increasing time are shown as a function of time. Region II with  $6 \times 6$   $\mu\text{m}^2$  was poled by  $-10$  V, and then part of Region I with  $3 \times 3$   $\mu\text{m}^2$  was reverse-poled by  $+10$  V. Finally Region III with  $9 \times 9$   $\mu\text{m}^2$  was poled, including the as-grown surface being scanned without dc bias (Fig. 5). The contrast of the images represents the relative polarization or charge density of the films. As shown in Fig. 5(a), Film A displays a quick disappearance of

TABLE II. The refinement lattice parameters of the BNT thin films.<sup>59</sup>

	a (Å)	b (Å)	c (Å)	Volume (Å <sup>3</sup> )	$R_{wp}$ (weighted profile R-factor)
Film A	5.43	5.39	32.87	963.3	11.079
Film B	5.39	5.36	32.72	945.6	12.150
Film C	5.41	5.38	32.77	952.9	9.776
Film D	5.38	5.36	32.68	942.2	11.159



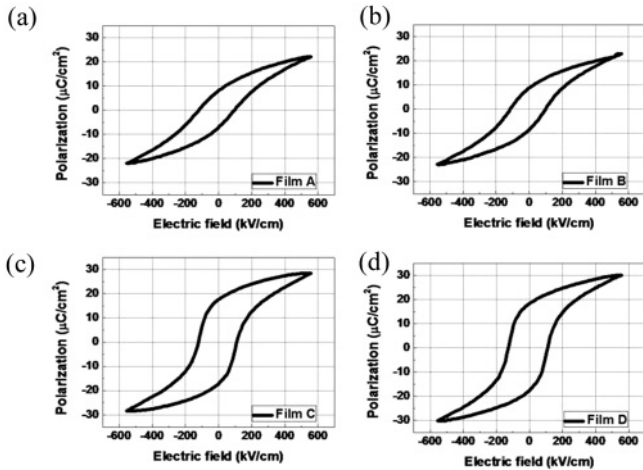


FIG. 3.  $P$ - $E$  loops of Film (a) A, (b) B, (c) C, and (d) D. This measurement was performed on a macroscopic scale by a TF analyzer. The films annealed in a fully oxygenated ( $PO_2 = 0.1$  MPa) showed higher remnant polarization than that of the films annealed in a  $N_2(80\%)/O_2(20\%)$  mixture with atmospheric pressure ( $PO_2 = 0.02$  MPa).

the boundaries among Regions I, II, and III. Recall that the Film A was less crystalline with some oxygen vacancies. It is reasonable to consider Film A to have weak polarization and mobile free charges. In Fig. 5(c) Film C shows a relatively slow vanishing of the boundaries as well as some fluctuations in Regions I and II. In the measurement of retention properties of ferroelectric thin films by PFM, the tip condition is very important; in this case it plays a role as a top electrode. Though the final topography was the same as the initial state, it was confirmed that the tip was not damaged throughout measurements.

Temporal changes for statistical distribution of each image pixel are plotted in Fig. 6. There is a pattern which is related to formation of polarized states and retention behaviors observed in the PFM images. The central part of all the PFM signals, which originates from the unpoled area in the images, is more or less off to the positive voltage bias, which means a built-in potential in the film. Depolarization field of the films partially makes up the asymmetric poling behavior, which is predominantly revealed in the ferroelectric thin films with no top metal electrodes. Figure 6(a) shows weak separation of poling and quick disappearance of the poled states of Film A. Figure 6(b) shows strong central and negatively biased peak and weak positively biased peak of Film B. In Fig. 6(c) Film C shows weaker separation and faster decay than Film B, even though Film C was annealed at a higher temperature and larger  $P_r$  values in its  $P$ - $E$  loop. Finally Film D shows retained polarization states of the films for both biased directions. The magnitude and population of the biased states are still asymmetric, but the states are relatively strong enough to tell retention of the polarization. From the previous analysis nurturing of polarization by external dc bias and holding-up of the states are strongly dependent on oxygen defects and crystallinity. Electrodynamics enlightening the phenomenological findings is very important to comprehend further technical applications of the materials.

#### IV. DISCUSSION

In the previous report<sup>35</sup> we have investigated the location of oxygen vacancy in BNT thin films depending on a different atmosphere in which metallic Bi peaks generated from breaking Bi-O bonds were observed from XPS measurements. The report has denoted metallic Bi peaks observed at 161.65 and 156.14 eV, while there was no shift and metallic Ti peaks. As a result, it has confirmed that perovskite structure of BNT has no oxygen vacancies because it has no metallic Ti peaks. From the results we could confirm that oxygen vacancies in BNT thin films were mainly positioned at the  $Bi_2O_2^{2+}$  layers and not at the perovskite substructure since substitution of Nd for Bi in the perovskite substructure stabilizes oxygen-ion bonding in the  $TiO_6^{8-}$  octahedral. Even though the possible sites of oxygen defects can be changed by annealing conditions, our experimental result has already been predicted by a theoretical work by Hashimoto *et al.*<sup>36</sup> The amount of oxygen vacancies by the area ratio of the Bi 4f core-level-fitted XPS spectra was estimated to be  $2.4 \pm 0.5\%$  for the BNT thin film annealed under 0.02 MPa, giving a formula of  $Bi_{3.15}Nd_{0.85}Ti_3O_{11.71}$ .<sup>35</sup> An x-ray absorption study on bismuth lanthanum titanate by Kim *et al.* shows the oxygen

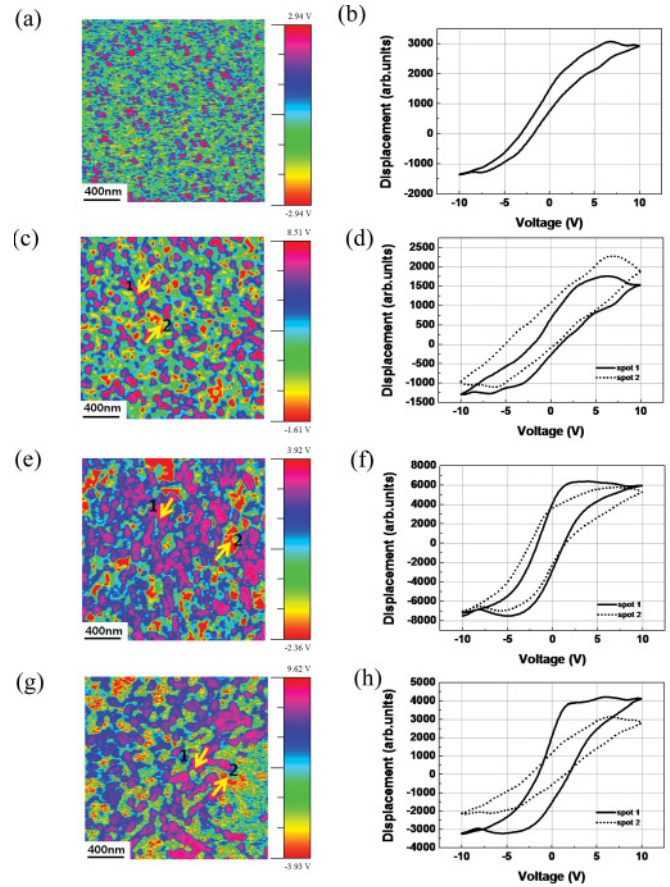


FIG. 4. (Color online) PFM images of Film (a) A, (c) B, (e) C, and (g) D. Local hysteresis loops of Film (b) A, (d) B, (f) C, and (h) D. The images and hysteresis were taken as grown state without external poling. The different contrast of arrows 1 and 2 in the images represented the opposite direction of polarization in each domain.

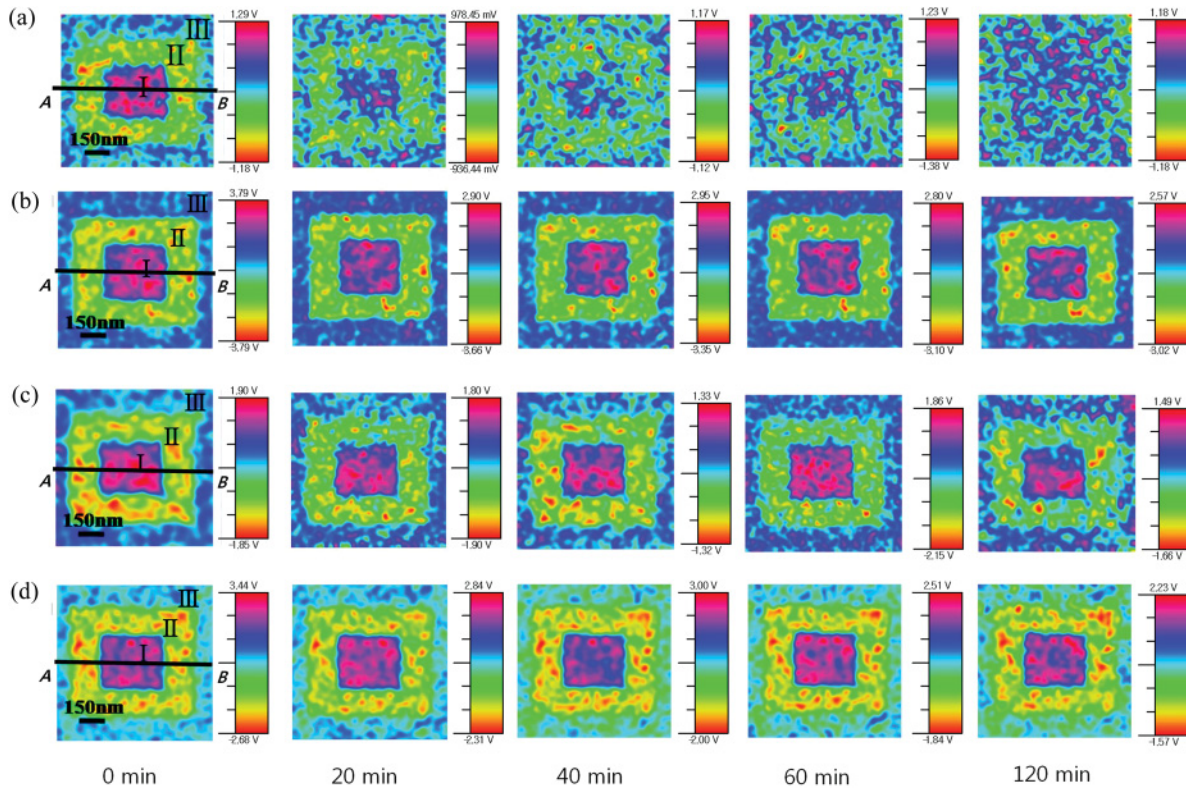


FIG. 5. (Color online) Time-dependent PFM images of Film (a) A, (b) B, (c) C, and (d) D. All the images were taken every four minutes, but the captured ones are 0, 20, 40, 60, and 120 min after reverse-poling scheme, respectively. The contrast was rescaled for each image; therefore, it does not represent relative strength of polarization.

bonding and shape of orbital are different in the perovskite and the  $\text{Bi}_2\text{O}_2^{2+}$  layers, most probably oxygen defects are formed at the  $\text{Bi}_2\text{O}_2^{2+}$  layers.<sup>37</sup> Thus, it is consistent with experimental

and theoretical reports of other's that our annealing conditions induce oxygen vacancies in the  $\text{Bi}_2\text{O}_2^{2+}$  layers since Nd strengthened the bonding of the perovskite structure.<sup>23</sup>

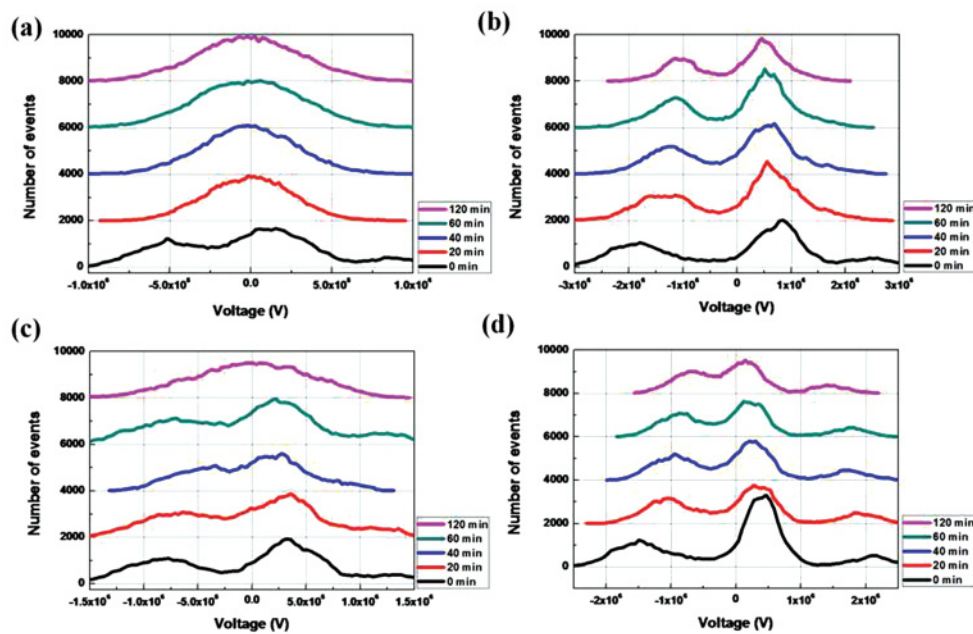


FIG. 6. (Color online) Temporal changes of polarized states of Film (a) A, (b) B, (c) C, and (d) D. All the graphs were extracted from the images in Fig. 5. The ordinate axis represents the number of events (i.e., pixels of the images) for each voltage response (i.e., PFM signal). The abscissa axis is the output voltage signal, which is interpreted as a piezoresponse of the ferroelectrics. All the profiles get smaller, or even fluctuating, when time evolves. This is another picture to look into time-evolution of the polarization in each poled region.



Though the films annealed in a fully oxygenated atmosphere showed a little bit higher remnant polarization than the films annealed in a  $N_2(80\%)/O_2(20\%)$  mixture, the significant difference was shown between the films with different annealing temperature in Fig. 3. When the annealing temperature increased, the remnant polarization also increased. The  $900^\circ\text{C}$  annealed film shows a well-saturated  $P$ - $E$  loop with larger  $P_r$ . This result indicates that domains in the films annealed in  $900^\circ\text{C}$  are switchable easily. The grain size of the film annealed in  $900^\circ\text{C}$  is larger than that of the  $800^\circ\text{C}$  annealed film (not shown here). Increase of the peak intensities and decrease of the peak width with increasing the annealing temperature are shown in the XRD results in Fig. 2. Domains could be switched easily in the large grains because domain walls in the small grains were stable under external field in the  $PbTiO_3$  thin films, as reported by Ren *et al.*<sup>38</sup> The amount of the domains, which are switched along the direction of the electric field, increase as the annealing temperature becomes increasing. It is similar to our results that the film annealed in  $900^\circ\text{C}$  has larger remnant polarization than the  $800^\circ\text{C}$  annealed film. Similar phenomena were also found in other bismuth layered ferroelectric thin films.<sup>39,40</sup> Therefore, increasing of crystallinity of the films can affect improvement of ferroelectric properties of the BNT thin films.

When we compare the effects of oxygen deficiencies on the increased lattice parameters and unit cell volume, we can clearly see that the films with more oxygen deficiency showed increased lattice parameters. In principle if the oxygen were extracted from  $Bi_2O_2^{2+}$  layers not from the perovskite structure, the unit cell would be not electrically neutral; therefore, there will be some vacancy in the parts of oxygen vacancy sites. In the case of Ag-doped  $SrBi_2Ta_2O_9$  (SBT) ferroelectrics, which are also members of the Aurivillius family with a general formula  $(Bi_2O_2)^{2+}(A_{m-1}B_mO_{3m+1})^2$  like BTO,  $Ag^+$  ions replace  $Bi^{3+}$  in the  $Bi_2O_2^{2+}$  layers. As a result, defective  $Bi_2O_2^{2+}$  layers are naturally present in SBT. The deficiency of  $Bi^{3+}$  in the  $Bi_2O_2^{2+}$  layers would increase the anionic repulsive forces between the layers of perovskite, giving rise to a larger lattice constant  $c$ .<sup>41</sup> Therefore, in our case of BNT with more oxygen vacancy, the deficient  $Bi_2O_2^{2+}$  layers could force the perovskite structure, which leads to increased lattice parameter  $c$  and unit cell volume. From the results of XRD and XPS<sup>35</sup> we suppose that oxygen vacancies were produced in  $Bi_2O_2^{2+}$  layers not from the perovskite layer in this structure. The oxygen vacancies act as space charges, and they could increase unit cell and degree of distortion.

Measurement of the remnant polarization in a macroscopic way as a function of time is well known to test retention and aging phenomena of the ferroelectric materials. However, a complete understanding is not achieved with this method, since most of the polarization evolution happens with interplay of defects inside the grains and grain boundaries at nanoscale. From the measured data presented previously with scanned probes, it is very interesting to draw some underlying electro-dynamics.

Over the last decade many groups have tried to understand the polarization switching and relaxation for several classes of ferroelectric materials. One of the pioneering works done by Gruverman *et al.* show domain formation and backswitching in  $Pb(Zr,Ti)O_3$  (PZT) thin films through measurement by PFM.<sup>42</sup>

Later, Ramesh and his colleagues elucidated some aspects of polarization kinetics in PZT with a new attempt of modeling with Johnson-Mehl-Avrami-Kolmogorov (JMAK) theory.<sup>43</sup> In their report they claimed that the JMAK model for phase-change kinetics in the epitaxial PZT films is successful to explain backswitching and reversal for  $180^\circ$  domain under constantly decaying imprint driving field. Also, faceting in the twin boundaries for low-indices plane-like (100) and (110) is a control factor for domain growth. Even though their work provides us a guideline for our study on BNT thin films, we found some fundamental distinctions between their work and ours. In PZT any oxygen defects are inevitably related to the bistable states of polarization, since the oxygen atoms are linked directly with the Ti atoms to form  $TiO_6^{-8}$  octahedra. It is important to keep in mind that BNT has two different locations, and chemical bonding of oxygen atoms and defects of oxygen do not lead to a direct deformation of the  $TiO_6^{-8}$  octahedra. In addition they studied epitaxial thin films where domains of the PZT grains are either  $90^\circ$  or  $180^\circ$ , which is much simpler than our polycrystalline BNT films.

Henceforth, it is worthwhile to look over polarization switching and relaxation on SBT in another important class of ferroelectric materials. Gruverman and Auciello have extensively studied domain formation and switching in SBT systems.<sup>44,45</sup> Structural similarities of SBT with BNT imply more possible common background for the electro-dynamics related to polarization than PZT. Highly anisotropic layered structure and direction of polarization in polycrystalline SBT films opens a possible inhomogeneous distribution of domain formation and switching phenomena. While a wide range of physical properties has been probed for SBT films by PFM, a systematic study for oxygen defects and crystallinity on polarization kinetics in SBT is lacking. It is likely that discovery of SBT was driven by inherent nature of strong binding of its perovskite,<sup>46</sup> while BNT was designed by deliberate addition of rare-earth atoms into perovskite structure in bismuth titanate, which is known to have poor fatigue properties.<sup>47</sup> This fatigue-free characteristic of SBT has been explained as a role of oxygen atoms in the  $Bi_2O_2^{2+}$  layers, which might also be a key factor for retention of polarization in BNT films.

Figure 7(a) shows a cross-sectional line profile of Film A in which the relaxation pattern looks very quick, as expected. Relaxation behaviors of these two regions look coincidental until 4000 sec, as shown in Fig. 8(a). After that time the two regions behave in a very different manner. The signals increase in a certain temporal zone for both single and reverse-poled regions, indicating that the charges move in and out of the regional boundaries. From this result it is reasonable to think that relaxation behaviors of Film A are dominated more by oxygen vacancy-related free charges rather than remnant ferroelectric polarization. The time-dependent charged states of Film C was shown in Fig. 7(c). As we expected from the PFM images, the polarization states look fluctuating. Since Film C was not grown at fully oxygenated ambient, it is necessary to consider oxygen vacancy-related charges in this case. The features on Region I and II in Fig. 5(b) look rigid over the measurement time in Film B, which is supposed to have less oxygen vacancies. This is indicating that the polarization of Film B was sustained. It is clear from the

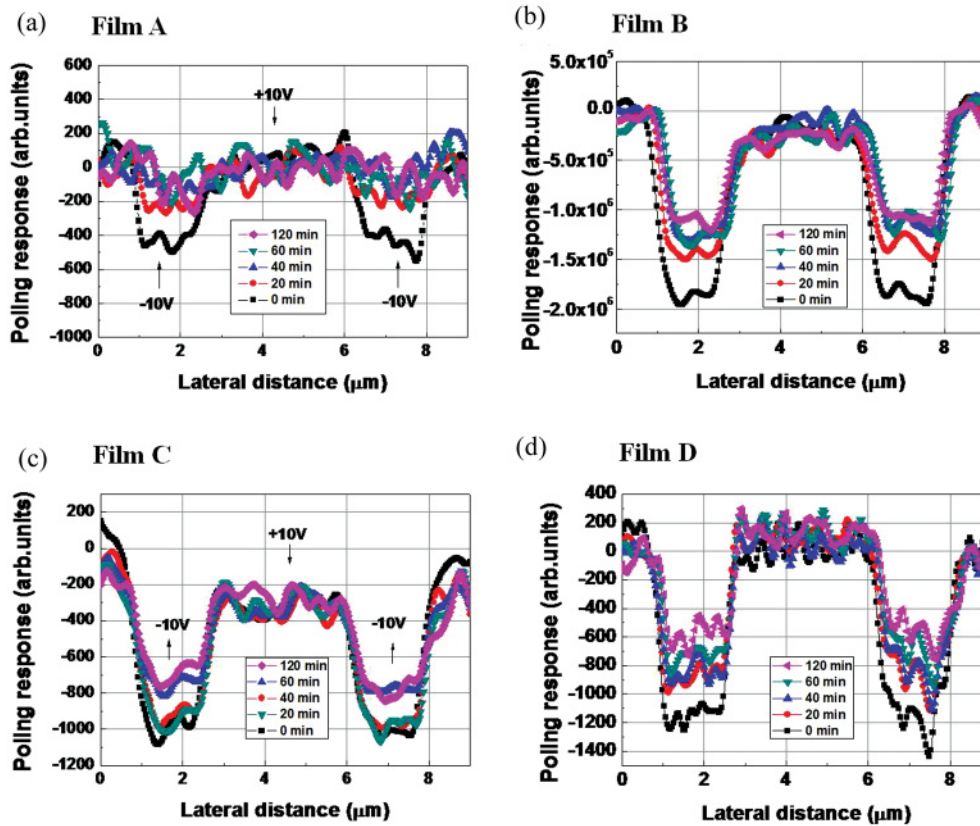


FIG. 7. (Color online) Cross-sectional line profile of the image across the *A-B* line of Film (a) A, (b) B, (c) C, and (d) D of the images in Fig. 5, respectively. The magnitude of poling response of both the single- and reversed-poled regions tends to decrease as time elapses. Even though the line profile does not fully guarantee all the decay behavior of the films, it does provide an overview of the time-dependence of polarization. In addition to time-dependent polarization in each poled section, the relative magnitude implies built-in potential or imprinted behaviors.<sup>25</sup>

images that Film C has faster relaxation of charges than Film B, which is an interesting guideline because oxygen vacancies are the most influential for retention of ferroelectric polarization. Figure 5(d) exhibits charge relaxation of Film D, which was grown with well-crystalline and fully oxygenized grains. As expected, Film D has substantial retention characteristics of charges and polarization.

Let us first consider the samples with simple decays of polarization. Areal average of Regions I, II, and III of Films B and D over the measurement time is displayed in Fig. 8. Numbers in the ordinate axis represent only relative values of the charges and the polarization acquired from the PFM images. As we previously demonstrated in earlier reports,<sup>24,25</sup> the reverse poling is effective to obtain retained states of polarization in ferroelectric thin films. Through the scheme, free charges are trapped, and domains tend to pin in the reverse-poled region. Relative values of polarization in Film D are larger than Film B. In addition the single-poled regions, as shown in Figs. 8(b) and 8(d), indicate that the relaxation of the remnant polarization is driven by a stretched exponential decay, a characteristic which has been observed in a variety of ferroelectric materials.<sup>24,25</sup> The mechanism may be described as

$$\Delta P = \Delta P_0 \exp[-\alpha t^n], \quad (1)$$

where  $t$  is the time,  $\alpha$  is a constant,  $\Delta P$  is polarization,  $\Delta P_0$  is polarization at  $t=0$ , and  $n$  is the characteristic number of a stretched exponential decay. A stretched exponential behavior with  $n < 1$  has been described as a dispersive transport and random-walk process.<sup>49</sup> For the reverse-poled region the characteristic exponent is found to be  $n_+ = 0.086$  and  $\alpha_+ = 0.026$  of Film B in Fig. 8(b) and that of Film D is  $n_+ = 0.289$  and  $\alpha_+ = 0.065$  in Fig. 8(d). The fit is empirical but important to estimate the relaxation in the ferroelectric materials. However, there had been no clear explanation of correlation between  $n$  value and crystallinity in a stretched exponential decay. In a disordered matrix it has been known that if the minority of crystallized regions decoupled, then the interaction effect will be to increase  $n$  values toward 1 in inorganic glasses.<sup>50</sup> Considering our result in different  $n$  values from the fitting curves in Films B and D, we suppose that there are more crystallized regions in Film D than that in Film B, and they will lead to a higher  $n$  value than that of Film B. This suggestion corresponds with the result of the rocking curves in Fig. 2. In our earlier reports we investigated the poling response of ferroelectric BLT thin films and relaxor ferroelectric  $\text{PbMg}_{1/3}\text{Nb}_{2/3}\text{O}_3\text{-PbTiO}_3$  (PMN-PT) thin films by the same reverse-poling scheme.<sup>24,25</sup> With the same layered structure BNT and BLT should have similar poling and relaxation behaviors. On the other hand the cubic perovskite PMN-PT has generally similar but unique

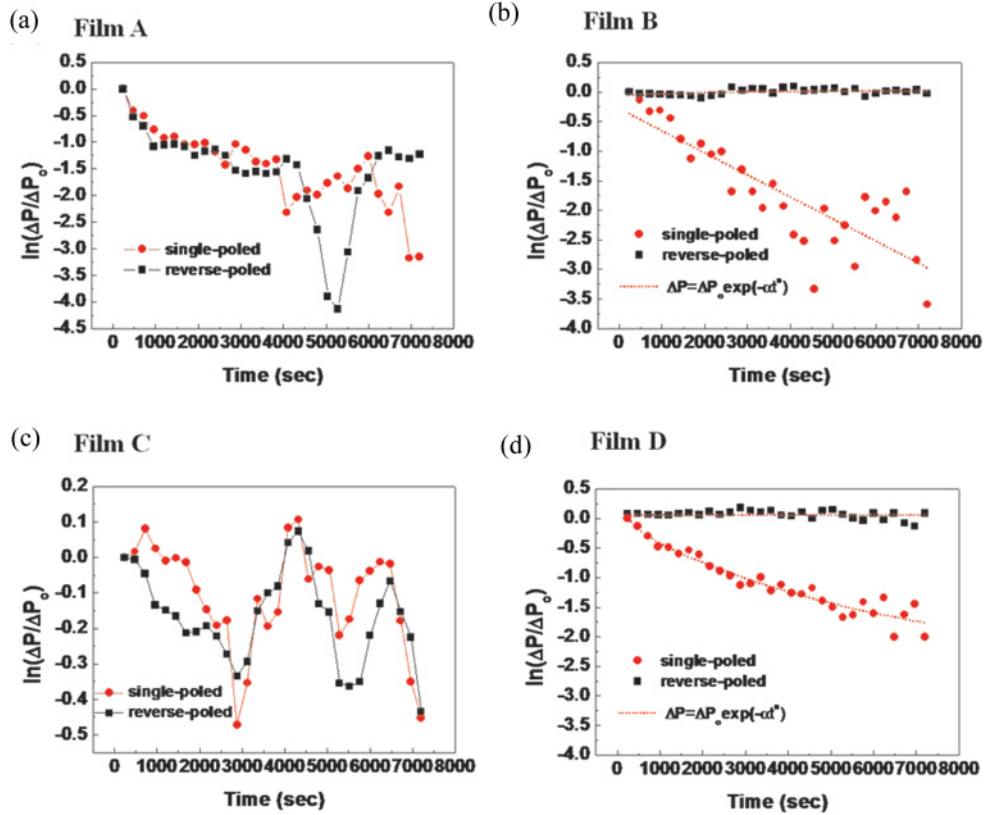


FIG. 8. (Color online) Plots of the *a real* average of poling response as a function of time of Film (a) A, (b) B, (c) C, and (d) D. A stretched exponential decay is a well-suited functional fitting form for the time dependence of the poled regions in Films B and D. The ordinate axes means that the difference between the polarization value at  $t = 0$  and obtained polarization as a function of time by PFM. [See Eq. (1).] Films A and C are not consistent with the decay model so a diffusive mechanism is applied to explain them.

fluctuation and changes in their temporal response. From the viewpoint of scaling theory the ferroelectric materials must show a universal constant in their relaxation. This may need another fundamental and extensive study, while our model will give a clue to it because the extended exponential decay is a random-walk distribution. It is important to investigate the poling and relaxation at nanoscale because there is not yet a unified explanation whether the characteristics are collective at short-range or long-range interaction. In the bulk crystal of BNT it has been investigated that domain clamping of  $90^\circ$  domains occurred for polarization switching by Kitanaka *et al.* BTO single crystals with less oxygen vacancies showed a low-volume fraction of the clamped  $90^\circ$  domain in which the remnant polarization decreased.<sup>17</sup> This result is consistent with our result, although in our thin films it is difficult to define  $90^\circ$  or  $180^\circ$  domains; the defective thin films showed a poor retention behavior and less remnant polarization.

Interpretation of the relaxation of polarization with the extended exponential decays or a modified version of a domain-growth theory has been adopted by many groups,<sup>42,43,51</sup> while there were still other attempts considering logarithmic decays due to mobile-free charges involved with a broad range of decay time.<sup>48,52</sup> Random field in relaxor ferroelectrics was also considered as a key origin for polarization relaxation with logarithmic distribution of characteristic decay time, which is determined by long-range breakdown of interaction and clustering of polar states.<sup>53</sup> Influence of depolarization field for

polarization relaxation is another factor to be considered. For ultrathin BaTiO<sub>3</sub> epitaxial thin films, a serious driving force to reverse polarization effectively due to the depolarization field was reported by Noh and his colleagues.<sup>54</sup> Owing to asymmetric electrodes for our BNT films, the same scheme of interpretation with depolarization field is not applicable, but it might be imperative to explore thickness dependence of domain clamping as a function of external dc bias.

Understanding of relaxation behaviors of Films A and C looks challenging because they tend to show random variations of PFM signals. If there is a ferroelectric polarization, which was confirmed by macroscopic and microscopic measurement of *P-E* loops, a monotonic decay of the polarization is expected regardless of the time dependence. Surge of charge states happened in both samples even though their timing does not look the same.<sup>55</sup> Repetitive measurement of the charged states in other spots in the same samples discloses the randomness of the upturn and decline. Oxygen defects are known to generate not only simple-point charge states but also combined states of atom vacancy.<sup>30</sup> Mobility of the defects across the poling regions between I and II or II and III is significant. Their behavior is not drifting due to electric potential, which can be generated by internal polarization and other unequal distribution of charges, but rather diffusion due to chemical potential of each region where the charges are barely trapped by external dc bias in oxygen-defect sites. A mathematical model to explain this diffusive trend in



oxygen-defected ferroelectrics is not yet established. However, diffusion phenomena prevail in disordered systems, including proton glasses,<sup>56</sup> spin glasses,<sup>57</sup> conducting polymers,<sup>58</sup> and recently graphene.<sup>59</sup> Implication of the diffusive behavior is also a signature by fractal formation because the artificial domain boundaries between Regions I and II or Regions II and III looks like a self-similar structure with no one-dimensional feature.<sup>60</sup> To clarify the nature of the disordered systems of oxygen-defective ferroelectrics, it will be crucial to get spectral dielectric functions of PFM signals.

## V. CONCLUSION

Introduction of oxygen vacancies into BNT thin films is performed simultaneously with control of crystallinity.

Oxygen vacancies seem to behave as mobile-free charges which show a quick declination in polarization of the BNT films measured by PFM. Charge redistribution could appear in more defective thin films with oxygen vacancies in  $\text{Bi}_2\text{O}_2^{+2}$  layers while less defective thin films can lead dielectric relaxation as exponential decay. Therefore, polarization states and their temporal retention behaviors are significantly influenced by oxygen vacancy and crystallinity in the BNT thin films.

## ACKNOWLEDGMENTS

This work was supported by the National Research Foundation of Korea (NRF) grant funded by the Korea government (MEST) (Quantum Metamaterials Research Center, Grant No. 2008-0062236).

\*Corresponding author: wmjo@ewha.ac.kr

<sup>1</sup>D.-H. Do, P. G. Evans, E. D. Isaacs, D. M. Kim, C. B. Eom, and E. M. Dufresne, *Nat. Mater.* **3**, 365 (2004).

<sup>2</sup>J. F. Scott, *Ferroelectric Memories* (Springer, Berlin, 2000), p. 4.

<sup>3</sup>J. F. Scott and C. A. Paz de Araujo, *Science* **246**, 1400 (1989).

<sup>4</sup>A. S. Mischenko, Q. Zhang, J. F. Scott, R. W. Whatmore, and N. D. Mathur, *Science* **311**, 1270 (2006).

<sup>5</sup>J. F. Scott, *Science* **16**, 954 (2007).

<sup>6</sup>B. G. Chae, Y. S. Yang, S. H. Lee, M. S. Jang, S. J. Lee, S. H. Kim, W. S. Baek, and S. C. Kwon, *Thin Solid Films* **410**, 107 (2002).

<sup>7</sup>W. L. Warren, D. Dimos, B. A. Tuttle, G. E. Pike, R. W. Schwartz, P. J. Clews, and D. C. McIntyre, *J. Appl. Phys.* **77**, 6695 (1995).

<sup>8</sup>I. K. Yoo and S. B. Desu, *Phys. Status Solidi A* **133**, 565 (1992).

<sup>9</sup>J. Lee and R. Ramesh, *Appl. Phys. Lett.* **68**, 484 (1996).

<sup>10</sup>D. Fu, K. Ishikawa, M. Minakata, and H. Suzuki, *Jpn. J. Appl. Phys.* **40**, 5683 (2001).

<sup>11</sup>V. C. Lo, *J. Appl. Phys.* **92**, 6778 (2002).

<sup>12</sup>B. H. Park, S. J. Hyun, S. D. Bu, T. W. Noh, J. Lee, H.-D. Kim, T. H. Kim, and W. Jo, *Appl. Phys. Lett.* **74**, 1907 (1999).

<sup>13</sup>W. L. Warren, B. A. Tuttle, and D. Dimos, *Appl. Phys. Lett.* **67**, 1426 (1995).

<sup>14</sup>H. M. Duiker, P. D. Beale, J. F. Scott, C. A. Paz de Araujo, B. M. Melnick, J. D. Cuchiaro, and L. D. McMillan, *J. Appl. Phys.* **68**, 5783 (1990).

<sup>15</sup>D. Dimos, H. N. Al-Shareef, W. L. Warren, and B. A. Tuttle, *J. Appl. Phys.* **80**, 1682 (1996).

<sup>16</sup>I. K. Yoo, S. B. Desu, and J. Xing, *Mater. Res. Soc. Symp. Proc.* **310**, 165 (1993).

<sup>17</sup>Y. Kitanaka, Y. Noguchi, and M. Miyayama, *Phys. Rev. B* **81**, 094114 (2010).

<sup>18</sup>Y. Noguchi, I. Miwa, Y. Goshima, and M. Miyayama, *Jpn. J. Appl. Phys.* **39**, L1259 (2000).

<sup>19</sup>Y. Noguchi, T. Matsumoto, and M. Miyayama, *Jpn. J. Appl. Phys.* **44**, L570 (2005).

<sup>20</sup>M. Takahashi, Y. Noguchi, and M. Miyayama, *Jpn. J. Appl. Phys.* **41**, 7053 (2002).

<sup>21</sup>S. E. Cummins and L. E. Cross, *J. Appl. Phys.* **39**, 2268 (1968).

<sup>22</sup>U. Chon, H. M. Jang, M. G. Kim, and C. H. Chang, *Phys. Rev. Lett.* **89**, 087601 (2002).

<sup>23</sup>T. Higuchi, Y. Noguchi, T. Goto, M. Miyayama, S. Shin, K. Kaneda, T. Hattori, and T. Tsukamoto, *Jpn. J. Appl. Phys.* **44**, L1491 (2005).

<sup>24</sup>T. Y. Kim, J. H. Lee, Y. J. Oh, M. R. Choi, and W. Jo, *Appl. Phys. Lett.* **90**, 082901 (2007).

<sup>25</sup>J. H. Lee, M. R. Choi, Y. J. Oh, and W. Jo, *Appl. Phys. Lett.* **91**, 072906 (2007).

<sup>26</sup>W. Jo, K. H. Kim, and T. W. Noh, *Appl. Phys. Lett.* **66**, 3120 (1995).

<sup>27</sup>F. Hou, M. Shen, and W. Cao, *Thin Solid Films* **471**, 35 (2005).

<sup>28</sup>J. Ma, X. M. Lu, Y. Kan, J. Gu, and J. S. Zhu, *J. Electroceram.* **21**, 837 (2008).

<sup>29</sup>T. Watanabe and H. Funakubo, *Jpn. J. Appl. Phys.* **39**, 5211 (2000).

<sup>30</sup>Y. Kitanaka, Y. Noguchi, and M. Miyayama, *Phys. Rev. B* **81**, 094114 (2010).

<sup>31</sup>K. Yamamoto, Y. Kitanaka, M. Suzuki, M. Miyayama, Y. Noguchi, C. Moriyoshi, and Y. Kuroiwa, *Appl. Phys. Lett.* **91**, 162909 (2007).

<sup>32</sup>M. Alexe, A. Gruverman, C. Harnagea, N. D. Zakharov, A. Pignolet, D. Hesse, and J. F. Scott, *Appl. Phys. Lett.* **75**, 1158 (1999).

<sup>33</sup>A. Gruverman, *Appl. Phys. Lett.* **75**, 1452 (1999).

<sup>34</sup>J. A. Christman, S.-H. Kim, H. Maiwa, J.-P. Maria, B. J. Rodriguez, A. I. Kingon, and R. J. Nemanich, *J. Appl. Phys.* **87**, 8031 (2000).

<sup>35</sup>R. H. Shin, J. H. Lee, G. Kim, W. Jo, D. H. Kim, H. J. Lee, and J. Kang, *Jpn. J. Appl. Phys.* **49**, 091501 (2010).

<sup>36</sup>T. Hashimoto and H. Moriwake, *Phys. Rev. B* **78**, 092106 (2008).

<sup>37</sup>D. W. Lee, J. W. Seo, S. Cho, S. R. Park, C. Kim, B. J. Kim, S.-J. Oh, B. S. Kang, T. W. Noh, and B. H. Park, *J. Appl. Phys.* **99**, 034101 (2006).

<sup>38</sup>S. B. Ren, C. J. Lu, J. S. Liu, H. M. Shen, and Y. N. Wang, *Phys. Rev. B* **54**, R14337 (1996); **55**, 3485 (1997).

<sup>39</sup>M. Nagata, D. P. Vijay, X. B. Zhang, and S. B. Desu, *Phys. Status Solidi A* **157**, 75 (1996).

<sup>40</sup>D. Wu, A. Li, T. Zhu, Z. Liu, and N. Ming, *J. Appl. Phys.* **88**, 5941 (2000).

<sup>41</sup>B. Sih, A. Jung, and Z.-G. Ye, *J. Appl. Phys.* **92**, 3928 (2002).

<sup>42</sup>A. Gruverman, H. Tokumoto, A. S. Prakash, S. Aggarwal, B. Yang, M. Wuttig, R. Ramesh, O. Auciello, and T. Venkatesan, *Appl. Phys. Lett.* **71**, 3492 (1997).

<sup>43</sup>C. S. Ganpule, A. L. Roytburd, V. Nagarajan, B. K. Hill, S. B. Ogale, E. D. Williams, and R. Ramesh, and J. F. Scott, *Phys. Rev. B* **65**, 014101 (2001).

<sup>44</sup>A. Gruverman and M. Tanaka, *J. Appl. Phys.* **89**, 1836 (2001).

- <sup>45</sup>O. Auciello, A. Gruverman, H. Tokumoto, S. A. Prakash, S. Aggarwal, and R. Ramesh, *MRS Bull.* **23**, 33 (1998).
- <sup>46</sup>C. A-Paz de Araujo, J. D. Cuchiaro, L. D. McMillan, M. C. Scott, and J. F. Scott, *Nature* **374**, 627 (1995).
- <sup>47</sup>B. H. Park, B. S. Kang, S. D. Bu, T. W. Noh, J. Lee, and W. Jo, *Nature* **401**, 682 (1999).
- <sup>48</sup>W. Jo, D. C. Kim, and J. W. Hong, *Appl. Phys. Lett.* **76**, 390 (2000).
- <sup>49</sup>S. Katayama, Y. Noguchi, and M. Miyayama, *Adv. Matter.* **19**, 2552 (2007).
- <sup>50</sup>J. C. Phillips, *Rep. Prog. Phys.* **59**, 1133 (1996).
- <sup>51</sup>C. S. Ganpule, V. Nagarajan, S. B. Ogale, A. L. Roytburd, E. D. Williams, and R. Ramesh, *Appl. Phys. Lett.* **77**, 3275 (2000); J. M. Benedetto, R. A. Moore, and F. B. McLean, *J. Appl. Phys.* **75**, 460 (1994).
- <sup>52</sup>D. Viehland and Y.-H. Chen, *J. Appl. Phys.* **88**, 6696 (2000).
- <sup>53</sup>D. J. Kim, J. Y. Jo, Y. S. Kim, Y. J. Chang, J. S. Lee, J. G. Yoon, T. K. Song, and T. W. Noh, *Phys. Rev. Lett.* **95**, 237602 (2005).
- <sup>54</sup>The nature of the physical quantities obtained by PFM is controversial at the present. It might be a mixture of mechanical response due to piezoelectricity and/or charge-charge interaction due to potential difference between the surface and the tip. In this text random changes of the PFM signals indicate that there might be something that is an itinerant carrier, mostly electrons or mobile ions. For simplicity of discussion we are using charged states rather than polarization for these samples.
- <sup>55</sup>U. Tracht, M. Wilhelm, A. Heuer, H. Feng, K. Schmidt-Rohr, and H. W. Spiess, *Phys. Rev. Lett.* **81**, 2727 (1998).
- <sup>56</sup>J. J. Torres, P. L. Garrido, and J. Marro, *Phys. Rev. B* **58**, 11488 (1998).
- <sup>57</sup>P. Phillips and H.-L. Wu, *Science* **252**, 1805 (1991).
- <sup>58</sup>A. Lherbier, B. Biel, Y. M. Niquet, and S. Roche, *Phys. Rev. Lett.* **100**, 036803 (2008).
- <sup>59</sup>V. B. Sapozhnikov and M. G. Goldiner, *J. Phys. A: Math. Gen.* **23**, 5309 (1990).
- <sup>60</sup>We used the reference lattice parameters in PDF #36-1486 ( $\text{Bi}_{3.6}\text{Nd}_{0.4}\text{Ti}_3\text{O}_{12}$ ) in which space group (SG) is *Cmmm* in this PDF reference; however, we assumed that SG of our case is *B2cb* because the symmetry was a little bit breaking by Nd-doping. And we also assumed that the atomic position was from ICSD ID 57337 ( $\text{Bi}_4\text{Ti}_3\text{O}_{12}$ ) and Nd would be substituted in Bi sites of perovskite structure.